Solid-State $^{31}P/^{27}Al$ and $^{31}P/^{23}Na$ TRAPDOR NMR Investigations of the Phosphorus Environments in Sodium Aluminophosphate Glasses†

David P. Lang,‡ Todd M. Alam,*,‡ and Denise N. Bencoe§

Organic Materials Department, Sandia National Laboratories, Albuquerque, New Mexico 87185-0888, and Materials Processing Department, Advanced Materials Laboratory, Sandia National Laboratories, 1001 University Boulevard SE, Albuquerque, New Mexico 87106

Received September 7, 2000. Revised Manuscript Received November 7, 2000

Solid-state $^{31}P/^{27}Al$ and $^{31}P/^{23}Na$ TRAPDOR NMR experiments have been used to investigate the spatial distribution of aluminum and sodium cations with respect to the phosphate backbone for a series of sodium aluminophosphate glasses, $x Al_2O_3 \cdot 50Na_2O \cdot (50-x)P_2O_5$ ($0 \leq x \leq 17.5$). From the $^{31}P/^{27}Al$ and $^{31}P/^{23}Na$ TRAPDOR data gathered, information about the medium-range order in these glasses was obtained. The expanded data allow for better identification and interpretation of the new resonances observed in the ^{31}P MAS NMR spectra with the addition of aluminum. The results of these experiments show that the sodium phosphate distribution remains relatively unchanged for the glass series and that the addition of aluminum occurs primarily through the modification of the phosphate tetrahedral backbone in the melt.

Introduction

The continued development of phosphate glasses for a variety of technologically important applications, including glass-to-metal seals[1,2] and laser hosts,[3,4] can be impeded by the low durability often associated with these materials. The addition of aluminum to simple phosphate glasses, however, has been shown to have a dramatic impact on their dissolution durability. For example, more than a 5 order reduction in the dissolution rate has been observed with a 15 molar percent (mol %) addition of Al_2O_3 to a sodium phosphate glass.[5] Thus, an understanding of the basic structural changes that occur with the addition of aluminum is important for the rational design of new glasses for specific applications.

In its crystalline form, P_2O_5 has a polymerized structure consisting of phosphorus tetrahedra with three bridging oxygen bonds (BO) and one terminal nonbridging oxygen bond (NBO).[6,7] Depolymerization of a glass network occurs when alkali-metal or alkaline-earth oxides (such as Na_2O, Li_2O, CaO) are added to the glass melt.[6,8] For example, when Na_2O is added, depolymerization results in the replacement of P−O−P linkages with the much weaker P−O−Na bonds.[5,9] Addition of aluminum oxide, Al_2O_3, to the melt also affects the glass network, but changes in the physical properties often imply that the structural polymerization has increased rather than decreased.[5,10]

Magic-angle spinning (MAS) nuclear magnetic resonance (NMR) spectroscopy has proven to be a valuable technique for probing the structural changes occurring in the evolution of binary or ternary phosphate glass systems.[11−13] When one-dimensional (1D) MAS NMR is used, differing local chemical environments for phosphorus and the modifier cations can often be discriminated and quantified. This short-range structural information allows for a better understanding of the physical properties of the glass, but gives little or no information about their structural arrangement or medium-range order (MRO). Structural variations in the MRO may also play a significant role in controlling the physical properties of a glass.

NMR techniques that utilize through-space dipole−dipole coupling between nuclei allow such spatial information to be established. The two-dimensional (2D) radio frequency dipolar recoupling (RFDR) experiment is one method for reintroducing magnetization exchange between homonuclear dipolar coupled spins and has

* To whom correspondence should be addressed. E-mail: sandia.gov.
† Sandia is a multiprogram laboratory operated by Sandia Corporation, a Lockheed Martin Company, for the United States Department of Energy under Contract DE-AC04-94AL85000.
‡ Organic Materials Department, Sandia National Laboratories.
§ Materials Processing Department, Sandia National Laboratories.

(1) Wilder, J. A. *J. Non-Cryst. Solids* **1980**, *38/39*, 879.
(2) Brow, R. K.; Kovacic, L.; Loehman, R. E. *Ceram. Trans.* **1996**, *70*, 177.
(3) Weber, M. J. *J. Non-Cryst. Solids* **1990**, *123*, 208.
(4) Payne, S. A.; Elder, M. L.; Campbell, J. H.; Wilke, G. D.; Weber, M. J.; Hayden, Y. T. *Ceram. Trans./Solid State Optic. Mater.* **1992**, *28*, 253.
(5) Brow, R. K. *J. Am. Ceram. Soc.* **1993**, *76*, 913.
(6) van Wazer, J. R. *Phosphorus and Its Compounds*; Interscience: New York, 1958; Vol. 1.
(7) Feike, M.; Graf, R.; Schell, I.; Jager, C.; Speiss, H. W. *J. Am. Chem. Soc.* **1996**, *118*, 9631.
(8) Martin, S. W. *Eur. J. Solid State Inorg. Chem.* **1991**, *28*, 163.
(9) Brow, R. K.; Kirkpatrick, R. J.; Turner, G. L. *J. Am. Ceram. Soc.* **1993**, *76*, 919.
(10) Kreidl, N. J.; Weyl, W. A. *J. Am. Ceram. Soc.* **1941**, *24*, 372.
(11) Eckert, H. *Prog. NMR Spectrosc.* **1992**, *24*, 159.
(12) Kirkpatrick, R. J.; Brow, R. K. *Solid State Nucl. Magn. Reson.* **1995**, *5*, 9.
(13) Brow, R. K. *J. Non-Cryst. Solids* **2000**, *263/264*, 1.

10.1021/cm000717l CCC: $20.00
Published on Web 01/05/2001

been used to probe the MRO between phosphorus nuclei.[14−17] Homonuclear multiple-quantum (MQ) experiments, which are more resolved than the RFDR spectra, have also been used to study the MRO in crystalline and glassy phosphate systems.[7,18−21] While the $^{31}P-^{31}P$ homonuclear magnetization exchange techniques provide information about the structural backbone of the phosphate systems, they do not yield any information about the proximity of phosphorus and the other network constituents, for example, ^{23}Na or ^{27}Al to ^{31}P. Such heteronuclear dipolar analysis is often complicated by the fact that the other constituents are quadrupolar nuclei ($I > {}^1/_2$), and the spin dynamics and magnitude of the quadrupolar interaction often require that unique NMR techniques be used.

Recently, several MAS-based NMR techniques were developed that utilize heteronuclear dipolar coupling between quadrupolar and spin-$^1/_2$ nuclei to ascertain connectivity and spatial interaction information. These include cross polarization (CP) involving quadrupolar nuclei,[22−24] rotational echo double resonance (REDOR),[25−27] transferred echo double resonance (TEDOR),[27,28] dipolar dephasing and transfer of populations double resonance (TRAPDOR),[29−32] rotational echo adiabatic passage double resonance (REAPDOR),[33] and dipolar exchange assisted recoupling (DEAR) experiments.[34] Many of these techniques have thus been employed and combined to acquire structural information in mixed quadrupolar, spin-$^1/_2$ nuclei systems including glasses,[17,35−42] zeolites,[27,31,32,43,44] and aluminophosphates.[45−51]

In this investigation we report the $^{31}P/^{27}Al$ and $^{31}P/^{23}Na$ NMR TRAPDOR results for the sodium aluminophosphate glass series, $x Al_2O_3 \cdot 50Na_2O \cdot (50-x)P_2O_5$ ($0 \le x \le 17.5$). Previously, Brow and Kirkpatrick[9] reported the 1D ^{31}P and ^{27}Al MAS NMR results for the glass series $x Al_2O_3 \cdot 50Na_2O \cdot (50-x)P_2O_5$ ($0 \le x \le 20$). Recently, Egan et al. also analyzed three glasses within this series, $x = 7.5$, 10, and 12.5 mol % aluminum, using a 2D heteronuclear CP correlation experiment to observe changes in $^{31}P/^{27}Al$ connectivity as the glass transforms from a metaphosphate to pyrophosphate composition.[41] In these previous investigations, the 1D ^{31}P MAS spectra clearly showed asymmetric resonances and shoulder features. Similar to Egan et al.,[41] subsequent NMR experiments within our laboratory revealed several new resolvable resonances appearing with the addition of aluminum. The results of the combined $^{31}P/^{27}Al$ and $^{31}P/^{23}Na$ TRAPDOR experiments described here allow the assignment of these new ^{31}P NMR resonances, along with a discussion of the role of sodium and aluminum in the MRO development for these glasses.

Experimental Procedures

Sample Preparation. Eight sodium aluminophosphate (NAP) glasses were prepared using a metaphosphate base glass ($NaPO_3$), α-Al_2O_3(99.99%), and sodium carbonate (Na_2CO_3) (assay 99.6%).[5] The metaphosphate base glass was prepared using technical-grade crystalline sodium hexametaphosphate $(NaPO_3)_6$, melted in a platinum crucible at 900 °C for 1 h. O_2 was bubbled in the melt (through a SiO_2 tube) for half the time and above the melt for the rest of the time. Quenching between two stainless steel plates produced thin pieces of glass that were then ground up with a steel mortar/pestle and put through a 1.18-mm sieve. All eight compositions were prepared with the same raw materials, melted in platinum crucibles, quenched in heated stainless steel molds, annealed for 1 h at ≈30°−40° above T_g, slow-furnace-cooled to room temperature, and stored in a desiccator. Glass compositions vary with 2.5 mol % increases in α-Al_2O_3. Individual glasses will be identified by their batch composition. For example, the label (50-5-45) for a NAP glass refers to the composition (in mol %) $50Na_2O \cdot 5Al_2O_3 \cdot 45P_2O_5$. A differential scanning calorimeter was used to measure the onset of glass transition (T_g) and glass crystallization (T_x) for each glass in the series.

NMR Experiments. All NMR spectra were collected on a Bruker AMX400 spectrometer modified to include a third, linearly amplified, radio frequency channel. The 1D MAS NMR

(14) Jäger, C.; Feike, M.; Born, R.; Spiess, H. W. *J. Non-Cryst. Solids* **1994**, *180*, 91.
(15) Born, R.; Feike, M.; Jäger, C.; Spiess, H. W. *Z. Naturforsch.* **1995**, *50*, 169.
(16) Alam, T. M.; Brow, R. K. *J. Non-Cryst. Solids* **1998**, *223*, 1.
(17) Hartmann, P.; Vogel, J.; Friedrich, U.; Jäger, C. *J. Non-Cryst. Solids* **2000**, *263/264*, 94.
(18) Feike, M.; Demco, D. E.; Graf, R.; Gotwald, J.; Hafner, S.; Speiss, H. W. *J. Magn. Reson. A* **1996**, *122*, 214.
(19) Feike, M.; Jager, C.; Spiess, H. W. *J. Non-Cryst. Solids* **1998**, *223*, 200.
(20) Hartmann, P.; Jana, C.; Vogel, J.; Jäger, C. *Chem. Phys. Lett.* **1996**, *258*, 107.
(21) Lee, Y. K.; Kurur, N. D.; Helmle, M.; Johannessen, O. G.; Nielsen, N. C.; Levitt, M. H. *Chem. Phys. Lett.* **1995**, *242*, 304.
(22) Blackwill, C. S.; Patton, R. L. *J. Phys. Chem.* **1984**, *88*, 6135.
(23) Vega, A. J. *J. Magn. Reson.* **1992**, *96*, 50.
(24) Vega, A. J. *Solid State NMR* **1992**, *1*, 17.
(25) Guillon, T.; Schaefer, J. *J. Magn. Reson.* **1989**, *81*, 196.
(26) Pan, Y.; Guillon, T.; Schaefer, J. *J. Magn. Res.* **1990**, *90*, 330.
(27) Fyfe, C. A.; Mueller, K. T.; Grondey, H.; Wong-Moon, K. C. *Chem. Phys. Lett.* **1992**, *199*, 198.
(28) Hing, A. W.; Vega, S.; Schaefer, J. *J. Magn. Reson.* **1992**, *96*, 205.
(29) van Eck, E. R. H.; Janssen, R.; Maas, W. E. J. R.; Veeman, W. S. *Chem. Phys. Lett.* **1990**, *174*, 428.
(30) Grey, C. P.; Veeman, W. S.; Vega, A. J. *J. Chem. Phys.* **1993**, *98*, 7711.
(31) Grey, C. P.; Vega, A. J. *J. Am. Chem. Soc.* **1995**, *117*, 8232.
(32) Fyfe, C. A.; Wong-Moon, K. C.; Huang, Y.; Grondey, H.; Mueller, K. T. *J. Phys. Chem.* **1995**, *99*, 8707.
(33) Guillon, T. *J. Magn. Reson. A* **1995**, *117*, 326.
(34) Sachleben, J. R.; Frydman, V.; Frydman, L. *J. Am. Chem. Soc.* **1996**, *118*, 9786.
(35) Herzog, K.; Thomas, B.; Sprenger, D.; Jäger, C. *J. Non-Cryst. Solids* **1995**, *190*, 296.
(36) van Wüllen, L.; Züchner, L.; Müller-Warmuth, W.; Eckert, H. *Solid State NMR* **1996**, *6*, 203.
(37) Schaller, T.; Rong, C.; Toplis, M. J.; Cho, H. *J. Non-Cryst. Solids* **1999**, *248*, 19.
(38) Wenslow, R. M.; Mueller, K. T. *J. Non-Cryst. Solids* **1998**, *231*, 78.
(39) Wenslow, R. M.; Mueller, K. T. *J. Phys. Chem. B* **1998**, *102*, 9033.
(40) Zeng, Q.; Nekvasil, H.; Grey, C. *J. Phys. Chem. B* **1999**, *103*, 7406.
(41) Egan, J. M.; Wenslow, R. M.; Mueller, K. T. *J. Non-Cryst. Solids* **2000**, *261*, 115.
(42) Prabakar, S.; Wenslow, R. M.; Mueller, K. T. *J. Non-Cryst. Solids* **2000**, *263/264*, 82.
(43) van Eck, E. R. H.; Veeman, W. S. *J. Am. Chem. Soc.* **1993**, *115*, 1168.
(44) Kao, H.-M.; Grey, C. *J. Phys. Chem.* **1996**, *100*, 5106.
(45) Rocha, J.; Lourence, J. P.; Ribeiro, M. F.; Fernandez, C.; Amoureux, J. P. *Zeolites* **1997**, *2/3*, 156.
(46) Fernandez, C.; Amoureux, J. P.; Chezeau, J. M.; Delmotte, L.; Kessler, H. *Microporous Mater.* **1996**, *6*, 331.
(47) Fernandez, C.; Delevoye, L.; Amoureux, J. P.; Lang, D. P.; Pruski, M. *J. Am. Chem. Soc.* **1997**, *119*, 6858.
(48) Pruski, M.; Lang, D. P.; Fernandez, C.; Amoureux, J. P. *Solid State NMR* **1997**, *7*, 327.
(49) Pruski, M.; Bailly, A.; Lang, D. P.; Amoureux, J. P.; Fernandez, C. *Chem. Phys. Lett.* **1999**, *307*, 35.
(50) Fernandez, C.; Lang, D. P.; Amoureux, J. P.; Pruski, M. *J. Am. Chem. Soc.* **1998**, *120*, 2672.
(51) Taulelle, F.; Pruski, M.; Amoureux, J. P.; Lang, D. P.; Bailly, A.; Huguenard, C.; Haouas, M.; Gérardin, C.; Loiseau, T.; Férey, G. *J. Am. Chem. Soc.* **1999**, *121*, 12148.

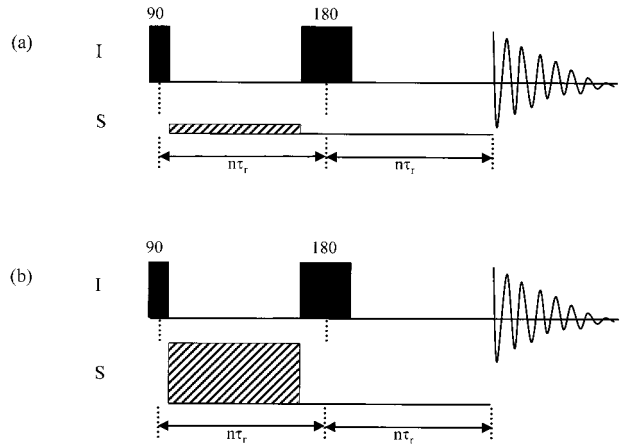

Figure 1. TRAPDOR pulse sequence is applied under MAS conditions with rotational period, τ_r. It consists of two parts: (a) a spin−echo acquired without S spin irradiation (due to high attenuation on the S channel amplifier) and (b) repeating the spin−echo experiment with application of a 50-kHz rf irradiating pulse to the S nuclei.

spectra of ^{27}Al and ^{31}P nuclei were collected using a 4-mm MAS broad-band triple-resonance probe and a spinning speed of 10 kHz. Spectra of aluminum were acquired at 104.271 MHz using a 4-μs π/6 pulse, 4096 signal averages, and a 0.5-s recycle delay. Spectra of phosphorus were acquired at 161.987 MHz using a 14.7-μs π/2 pulse, 32−512 signal averages, and a recycle delay of 120 s. As the samples studied are anhydrous, no ^{1}H decoupling was applied. The ^{27}Al and ^{31}P NMR shifts are reported using the δ scale, with positive values being downfield, and are referenced to 1 M $Al(OH_2)_6^{3+}$ ($\delta = 0.0$ ppm) and $(NH_4)H_2PO_4$ ($\delta = 0.8$ ppm with respect to 85% H_3PO_4 $\delta = 0.0$), respectively.

TRAPDOR NMR experiments (see Figure 1) were used to measure the heteronuclear dipolar interactions between the I (^{31}P) and S (^{27}Al or ^{23}Na) spins within the glass. This information was acquired by measuring the difference of the spin−echo of the I nuclei obtained with and without irradiation of the S nuclei during part of the pulse sequence.[29−32] The continuous irradiation of the S nuclei during *n* rotor periods modifies the Zeeman population levels of the S spin, which in turn affects the magnetization of the ^{31}P nuclei dipolar coupled to it. This interference thus alters the refocusing of the ^{31}P spin−echo in the pulse sequence. The TRAPDOR difference spectrum, ΔS, was obtained by subtracting the Fourier-transformed spectra of the two experiments with and without decoupling. The TRAPDOR experiments were performed using a 4-mm MAS broad-band triple-resonance probe with a sample rotation of 10 kHz. A 162 ± 10 MHz band-pass filter was utilized on the ^{31}P channel and a 102 ± 10 MHz band-pass filter on the ^{23}Na (or ^{27}Al) channel. NMR resonance frequencies were 161.987 MHz for ^{31}P, 104.271 MHz for ^{27}Al, and 105.849 MHz for ^{23}Na. The ^{31}P π/2 pulse was 17.5 μs, corresponding to a rf field strength of 14.3 kHz and was applied with minimal offset. To minimize variations in experimental conditions and eliminate spectrometer timing artifacts, the ^{27}Al or ^{23}Na decoupling pulse on the S nuclei was triggered in both experiments with minimal offset,[32] from very high (120 dB) attenuation for no S irradiation to low (12 dB) for maximum S irradiation. As the ^{31}P π/2 and π pulses were synchronized with the rotor period, the length of the decoupling pulse varied from 4 to 100 rotor cycles (0.4−10 ms). At higher rf amplitudes (lower attenuation values) the effects of the dephasing difference spectrum are maximized. When ≈50 kHz of rf power on the ^{23}Na (or ^{27}Al) channel (υ_{rf}) and a 10 kHz MAS speed (υ_R) is used, the TRAPDOR effect is observable and the chemical shift anisotropy of the ^{31}P nuclei is reduced enough to appreciably separate the unique phosphorus environments. As our results did not necessitate it, the quadrupole coupling constants of ^{23}Na and ^{27}Al were not determined, although such calculations are possible in the TRAPDOR experiment.[31,40] Finally, as the difference between the resonance frequencies of ^{27}Al and ^{23}Na is rather small (1.6 MHz for our field strength), the possibility of the irradiation of ^{27}Al affecting ^{23}Na, or vice versa, was investigated. A trial ^{31}P/^{27}Al TRAPDOR experiment performed on the 50-0-50 glass, which contains no aluminum, and involving irradiation of ^{27}Al during 20 rotor cycles yielded a null difference, ΔS, spectrum as expected. Similarly, a trial ^{31}P/^{23}Na TRAPDOR experiment performed on $AlPO_4$, which contains no sodium, showed no TRAPDOR difference effect either. These null experiments clearly demonstrate that the observed TRAPDOR effects are not due to low-frequency isolation between the sodium and aluminum, but result directly from heteronuclear dipolar interactions.

Results

All eight sodium aluminophosphate glasses were examined by a variety of NMR techniques. One-dimensional ^{31}P and ^{27}Al MAS NMR allow observation of the systematic changes occurring in the structure of the glass with increasing molar percent of aluminum. Information about the relative spatial distribution of phosphorus and aluminum, or phosphorus and sodium, was obtained using ^{31}P/^{27}Al and ^{31}P/^{23}Na TRAPDOR experiments, respectively. We will designate the aluminophosphate structures using a $Q^n(m\text{Al})$ notation, where *n* is the number of P next-nearest-neighbor (NNN) per P tetrahedron and *m* is the number of Al NNN per P. Thus, the crystalline compound $Al(PO_3)_3$ is described by a $Q^2(2\text{Al})$ phosphate structure,[52] $AlPO_4$ has a $Q^0(4\text{Al})$ structure,[53] and $KAlP_2O_7$ has a $Q^1(3\text{Al})$ structure.[54] Note that this notation makes no distinction as to the coordination number of aluminum and that the value of *n* represents only the number of bridging oxygens to other phosphorus atoms, not bridging oxygens as a whole, for example, Q^n.[56,57] Because we are not able to distinguish the aluminum coordination number in our TRAPDOR experiments, we will use the $Q^n(m\text{Al})$ notation for all subsequent discussions.

^{31}P MAS NMR. The 1D ^{31}P MAS NMR spectra of the NAP glasses are shown in Figure 2, with the evolution of the glass system with increasing molar percent of aluminum being readily seen. Because of site overlap and inhomogeneous broadening, deconvolution of the spectrum into individual sites is difficult. However, with the procedures of Herzfeld and Berger[55] and the results of our TRAPDOR experiments, attempts were made to deconvolute the entire MAS NMR sideband manifold of each spectrum and best "fit" them to unique phosphorus environments. Changes in the ^{31}P isotropic chemical shift values can be understood from the known relationships between the NNN bonding environments of P and comparison to the ^{31}P chemical shifts of model phosphate and aluminophosphate structures.[9] The ^{31}P isotropic chemical shift value for each site and its fractional population as a function of the molar percent of aluminum are listed in Table 1. The general trend for the

(52) van der Meer, H. *Acta Crystallogr. Sect. B* **1976**, *32*, 2423.
(53) Thong, N.; Schwarzenbach, D. *Acta Crystallogr. Sect. A* **1979**, *35*, 658.
(54) Ng, H. N.; Calvo, C. *Can. J. Chem.* **1973**, *51*, 2613.
(55) Herzfeld, J.; Berger, A. E. *J. Chem. Phys.* **1980**, *73*, 6021.
(56) Brow, R. K.; Phifer, C. C.; Turner, G. L.; Kirkpatrick, R. J. *J. Am. Ceram. Soc.* **1991**, *74*, 1287.
(57) Brow, R. K.; Kirpatrick, R. J.; Turner, G. L. *J. Non-Cryst. Solids* **1990**, *116*, 39.

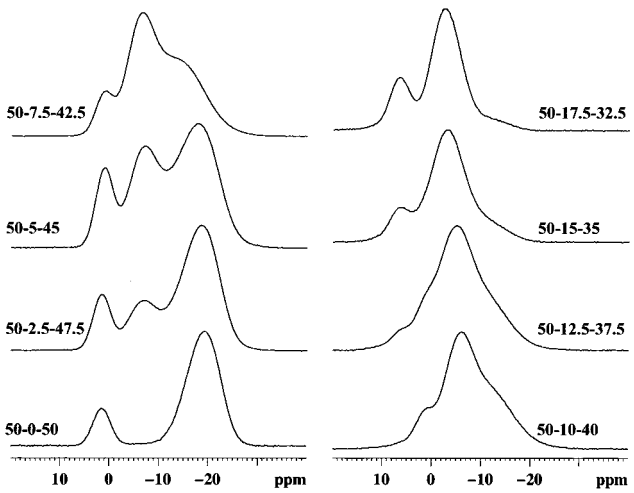

Figure 2. ^{31}P MAS NMR spectra of NAP glasses with molar percent composition $50Na_2O{\cdot}xAl_2O_3{\cdot}(50-x)P_2O_5$ ($0 \le x \le 17.5$).

Table 1. ^{31}P Isotropic Chemical Shift Assignments, Relative Populations, and T_g Data for the NAP Glass Series

NAP glass composition[a]	bond type[b]	δ_{iso} (ppm)[c]	$P_Q{}^{n}$ [d]	T_g[e] (°C)	T_x[f] (°C)
50-0-50	$Q^2(0Al)$	−19.3	0.90	287	343
	$Q^1(0Al)$	+1.5	0.10		
50-2.5-47.5	$Q^2(0Al)$	−18.7	0.70	301	406
	$Q^1(0Al)$	+1.6	0.10		
	$Q^1(1Al)$	−7.1	0.20		
50-5-45	$Q^2(0Al)$	−18.9	0.57	323	431
	$Q^1(0Al)$	+1.2	0.11		
	$Q^1(1Al)$	−6.4	0.24		
	$Q^1(2Al)$	−13.6	0.08		
50-7.5-42.5	$Q^2(0Al)$	−18.8	0.10	390	479
	$Q^1(0Al)$	+1.3	0.09		
	$Q^1(1Al)$	−5.9	0.44		
	$Q^1(2Al)$	−13.6	0.37		
50-10-40	$Q^1(0Al)$	+1.6	0.10	393	447
	$Q^1(1Al)$	−5.4	0.48		
	$Q^1(2Al)$	−12.0	0.42		
50-12.5-37.5	$Q^1(0Al)$	+1.6	0.09	368	425
	$Q^1(1Al)$	−5.5	0.16		
	$Q^1(2Al)$	−9.6	0.44		
	$Q^0(1Al)$	+6.3	0.06		
	$Q^0(2Al)$	−2.7	0.25		
50-15-35	$Q^1(2Al)$	−9.5	0.24	350	415
	$Q^0(1Al)$	+6.3	0.14		
	$Q^0(2Al)$	−2.7	0.62		
50-17.5-32.5	$Q^1(2Al)$	−9.3	0.11	358	405
	$Q^0(1Al)$	+6.7	0.20		
	$Q^0(2Al)$	−2.5	0.69		

[a] Batch composition: e.g., a glass labeled 50-10-40 is batched (in mol %) as $50Na_2O{\cdot}10Al_2O_3{\cdot}40P_2O_5$. [b] Bond types: e.g., notation $Q^2(0Al)$ denotes that each P has two bridging bonds to other phosphorus nuclei and zero bridging bonds to aluminum nuclei. [c] Isotropic chemical shift referenced to a secondary external reference $(NH_4)H_2PO_4$ (δ = 0.8 ppm with respect to phosphoric acid, δ = 0.0 ppm). [d] Fractional population, obtained from simulation of the entire MAS NMR sideband manifold (± 0.05). [e] Onset of glass transition temperature measured by DSC. [f] Onset of crystallization measured by DSC.

weighted average of the ^{31}P chemical shift values reported here are consistent with those reported by Brow et al.[9]

The ^{31}P NMR spectrum of the sodium metaphosphate base glass, 50-0-50 (Figure 2), displays the presence of $Q^2(0Al)$ (two bridging POP bonds per P) and $Q^1(0Al)$ (one bridging POP bond per P) phosphorus tetrahedral environments. Two structural designs consistent with such a spectrum are of a linear chain of $Q^2(0Al)$ species terminated by $Q^1(0Al)$ end groups or of cyclic structures of $Q^2(0Al)$ species existing concomitantly with a concentration of $Q^1(0Al)$ diphosphate species. A radio frequency dipolar recoupling experiment (RFDR) performed on this sample (data not shown) supports the first scenario, as prominent exchange cross-peaks indicate dipolar coupling between the $Q^2(0Al)$ and $Q^1(0Al)$ species. This observation is consistent with similar 2D RFDR investigations of lithium phosphate glasses.[16] The presence of such dipolar coupling would not exist if the species were isolated from one another, as would be predicted in the second structural scenario.[19] The existence of a significant $Q^1(0Al)$ fraction within the 50-0-50 spectrum indicates that the composition of the sodium metaphosphate base glass used in this study is modifier-rich, Na/P > 1. With equations developed by Van Wazer,[6,12] the nominal molar composition of our base glass is calculated at 52.4-0-47.6 rather than the assumed 50-0-50. The loss of P_2O_5 occurs during the glass preparation process when high melting temperatures are used.[5,56] This base glass was used in the preparation of all the remaining compositions.

Addition of α-Al_2O_3 to the $NaPO_3$ base glass results in the formation of two new phosphorus environments, a prominent one with a ^{31}P chemical shift at approximately −7 ppm and a smaller resonance at approximately −14 ppm. The creation of these environments reduces the fractional population of $Q^2(0Al)$ tetrahedral species, but diminishes the $Q^1(0Al)$ species only negligibly until the molar percent of aluminum is ≥10 (see Figure 2 and Table 1). For example, the ^{31}P spectrum of the 50-2.5-47.5 glass has a new isotropic phosphorus resonance at −7.1 ppm, while the $Q^2(0Al)$ resonance has shifted downfield by ≈0.6 ppm, and the chemical shift and concentration of the $Q^1(0Al)$ resonance remains nearly unchanged. The new phosphorus resonance at −7.1 ppm is attributed to the replacement of $Q^2(0Al)$ POP environments with POAl environments, $Q^1(mAl)$ m = 1, 2.[9,57] As the molar percent of aluminum increases, the concentration of $Q^1(mAl)$ species also increases while the concentration of $Q^2(0Al)$ species decreases. For example, in the 50-7.5-42.5 glass the $Q^2(0Al)$ species are no longer resolved; rather, both the $Q^2(0Al)$ and the $Q^1(0Al)$ resonance, to a lesser extent, exist as shoulder features on the upfield and downfield sides of the $Q^1(mAl)$ resonance(s), respectively. The conversion of the $Q^2(0Al)$ environments to $Q^1(mAl)$ m = 1, 2 environments continues through 10 mol % aluminum, at which time the concentration of $Q^2(0Al)$ species is negligible. The ^{31}P spectrum of the 50-10-40 glass consists of a broad asymmetric, upfield tailing $Q^1(mAl)$ resonance and a smaller downfield resonance. The downfield shoulder is due to a remaining fraction of $Q^1(0Al)$ end groups. Additional aluminum further modifies the glass, reduces the shielding on the phosphorus sites, and results in the formation of alumino orthophosphate, $Q^0(mAl)$, species. In the 50-12.5-37.5 glass, the $Q^1(0Al)$ species is no longer the dominant resonance downfield; rather, the alumino orthophosphate species, $Q^0(2Al)$ resonance at −2.8 ppm and

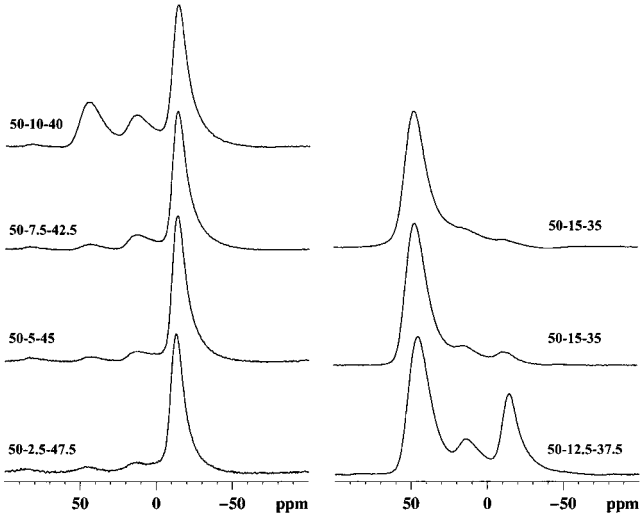

Figure 3. ^{27}Al MAS NMR spectra of NAP glasses with molar percent composition $50Na_2O{\cdot}xAl_2O_3{\cdot}(50-x)P_2O_5$ ($0 \le x \le 17.5$).

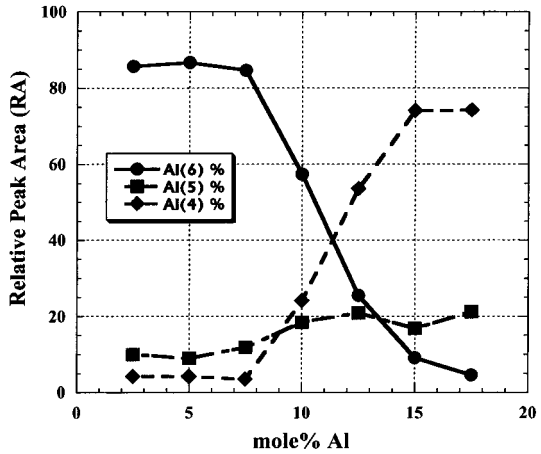

Figure 4. Percent of aluminum existing in each coordination state (RA) as a function of the molar percent of aluminum in the NAP glass series.

$Q^0(1Al)$ resonance at +6.3 ppm, are now present.[9,58] In the 50-15-35 and 50-17.5-32.5 glasses, the majority of the $Q^1(mAl)$ species have been replaced by $Q^0(mAl)$ species (see Table 1). Changes in the phosphorus spectra coincide with those occurring in the ^{27}Al MAS NMR spectra and will be discussed below.

^{27}Al MAS NMR. The results of the 1D ^{27}Al MAS NMR experiments of the NAP glasses are shown in Figures 3 and 4 and Table 2. All the NAP glasses have some fraction of four-coordinated, Al(4), five-coordinated, Al(5), and six-coordinated, Al(6), aluminum. The value of the chemical shift and the relative peak area (RA) of each Al environment for the NAP glass series are given in Table 2 and are consistent with those reported by Brow et al.[9] Note that the values listed in Table 2 do not take into account the quadrupolar effects of the aluminum nuclei. These effects will shift a resonance from its true isotropic value and result in a loss of signal intensity, introducing an error into the measured coordination percentages. However, as the most important parameter for this study is variation in the coordination of Al as the molar percent of aluminum changes, the error introduced by the quadrupole effects are small.

Table 2. Relative Peak Area (RA) and Chemical Shift Values for Al(4)-, Al(5)-, and Al(6)-Coordinated Aluminum as a Function of Molar Percent of Aluminum

NAP glass composition	Al(6) δ_{ppm}	Al(5) δ_{ppm}	Al(4) δ_{ppm}
50-2.5-47.5	−13.7	11.4	44.6
50-5-45	−13.0	11.5	42.9
50-7.5-42.5	−14.7	11.7	43.0
50-10-40	−14.6	12.8	43.4
50-12.5-37.5	−13.7	14.0	45.0
50-15-35	−12.1	14.8	46.0
50-17.5-32.5	−12.3	18.0	46.0

NAP glass composition	Al(6) RA	Al(5) RA	Al(4) RA
50-2.5-47.5	0.86	0.10	0.04
50-5-45	0.87	0.09	0.04
50-7.5-42.5	0.85	0.12	0.03
50-10-40	0.57	0.18	0.25
50-12.5-37.5	0.25	0.21	0.54
50-15-35	0.09	0.17	0.74
50-17.5-32.5	0.05	0.21	0.74

The dominant aluminum coordination is Al(6) at $x \le$ 7.5 mol % α-Al_2O_3 (see Figure 3). For the 50-2.5-47.5 glass the ratio of aluminum environments is ≈86% Al(6), 10% Al(5), and 4% Al(4). With increasing molar percent of α-Al_2O_3, the preferred Al coordination changes dramatically from octahedral to tetrahedral (see Figures 3 and 4). The 50-15-35 glass has nearly 75% Al(4) environments and only 9% Al(6) environments. The amount of five-coordinated aluminum, Al(5), also increases as α-Al_2O_3 is added, but levels off at ≈20% at $x \ge$ 10 mol % α-Al_2O_3.

^{31}P/^{27}Al TRAPDOR NMR. ^{31}P/^{27}Al TRAPDOR experiments were performed on each of the NAP glasses, with variation of the TRAPDOR signal as a function of ^{27}Al irradiation time (ranging from 0.4 to 10.0 ms) being shown in Figure 5a. Calculating the initial slope of these TRAPDOR curves for a short irradiation time (2 ms) produces a linear variation versus molar percent of aluminum as seen in Figure 5b.

The ^{31}P/^{27}Al TRAPDOR NMR spectra of the 50-2.5-47.5 NAP glass are shown in the left-hand column of Figure 6. The ^{31}P reference spectrum, which is analogous to a Hahn echo experiment with $\tau = 5$ ms (i.e., no ^{27}Al irradiation), is shown at the top. The middle spectrum displays the results of the experiment with ≈50 kHz of irradiation applied to the ^{27}Al nuclei throughout the dephasing time (τ). Subtraction of the middle spectrum from the reference spectrum yields the so-called TRAPDOR difference (ΔS) spectrum shown at the bottom. Clearly, the aluminum incorporated to form the 50-2.5-47.5 glass is preferentially coordinated to the new ^{31}P resonance at $\delta = -7.1$ ppm. This can be assigned to either a $Q^1(1Al)$ or $Q^1(2Al)$ phosphorus environment.[9,12,57,58] The effects of the ^{27}Al irradiation during the TRAPDOR experiment also influences the $Q^2(0Al)$ or upfield phosphorus resonance, but has no effect on the $Q^1(0Al)$ resonance. This is supported by the 1D ^{31}P MAS NMR results as well, which shows a small change in the chemical shift of the $Q^2(0Al)$ resonance as the molar percent of aluminum increases, while the chemical shift of the $Q^1(0Al)$ resonance stays relatively constant (see Table 1). The ^{31}P/^{27}Al TRAPDOR

(58) Dollase, W. A.; Merwin, L. H.; Sebald, A. *J. Solid State Chem.* **1989**, *83*, 140.

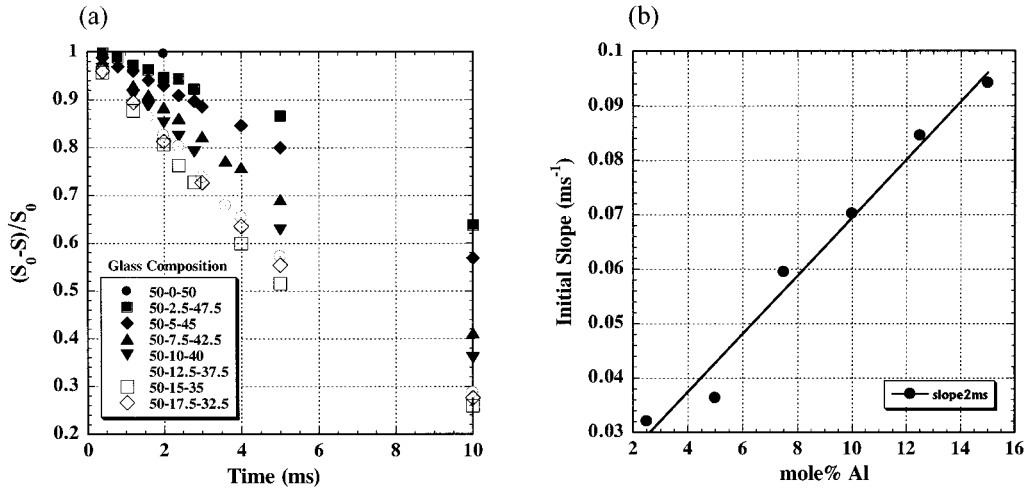

Figure 5. (a) $^{31}P/^{27}Al$ TRAPDOR difference amplitudes versus decoupling pulse duration, τ. The $^{31}P/^{27}Al$ interaction scales proportionally as the molar percent of aluminum increases. In (b) the slope of the initial TRAPDOR curves (2 ms) shown in (a) are plotted versus the molar percent of aluminum. The linear variation argues against Al or Al/Na segregation.

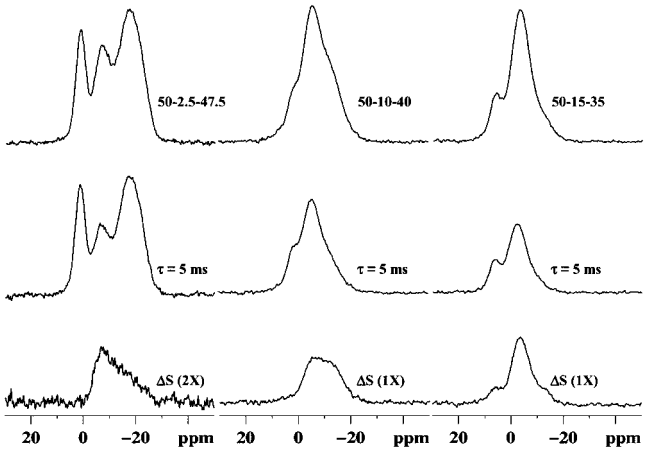

Figure 6. $^{31}P/^{27}Al$ TRAPDOR results of the 50-2.5-47.5 (left), 50-10-40 (middle), and 50-15-35 (right) NAP glasses. The top spectra are acquired without irradiation of the ^{27}Al nuclei. The spectra in the center were acquired with 50 kHz of irradiation applied to the ^{27}Al nuclei. The bottom spectra show the TRAPDOR difference, ΔS, for $\tau = 5$ ms resulting from each experiment.

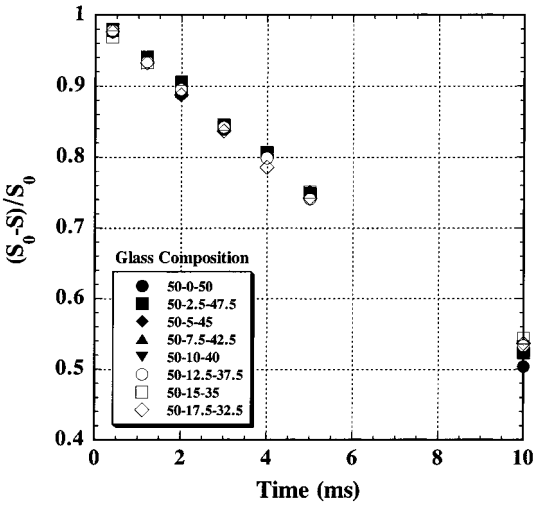

Figure 7. $^{31}P/^{23}Na$ TRAPDOR difference amplitudes versus decoupling pulse duration, τ. The relatively constant slope for the entire NAP glass series implies that the addition of ^{27}Al does not result in the extensive displacement of ^{23}Na by ^{27}Al.

experiment of the 50-10-40 glass is shown in the middle column of Figure 6, the arrangement of the spectra being analogous to those of the 50-2.5-47.5 glass. Once again, the aluminum incorporated into the glass shows a large TRAPDOR effect with the $Q^1(m\text{Al})$ species, but no effect with the $Q^1(0\text{Al})$ species. Finally, the $^{31}P/^{27}Al$ TRAPDOR experiment for the 50-15-35 glass is shown in the right-hand column of Figure 6. No longer are the effects of irradiating the ^{27}Al nuclei during the dephasing time τ specific to a few phosphorus environments; rather, all the phosphorus environments in this glass are affected, with a slight preference to the upfield resonances.

$^{31}P/^{23}Na$ TRAPDOR NMR. $^{31}P/^{23}Na$ TRAPDOR experiments were performed on all of the NAP glasses studied with ^{23}Na irradiation times ranging from 0.4 to 10 ms as shown in Figure 7. A relatively constant TRAPDOR decay for the entire NAP glass series was observed up to 10 ms of irradiation (Figure 7). To address the possible impact of ionic motion, and perhaps better resolve the various ^{31}P environments dipolar coupled to ^{23}Na, $^{31}P/^{23}Na$ TRAPDOR experiments were also performed at a lower temperature, 200 K. The TRAPDOR difference spectra, ΔS, generated at 200 K, however, are indistinguishable versus those at ambient temperature, suggesting that ionic motion has minimal impact at 200 K. The results presented here utilize experiments performed at ambient temperature.

Spectra from the $^{31}P/^{23}Na$ TRAPDOR experiments for the 50-2.5-47.5, 50-10-40, and 50-15-35 glasses at $\tau = 3$ ms are shown in Figure 8; the layout is the same as that in Figure 6. In these TRAPDOR experiments, all of the ^{31}P environments are affected by the ^{23}Na irradiation. As the molar percent of sodium is constant (50%) throughout this entire glass series, few, if any, structural bonding scenarios of phosphorus without proximity to sodium are expected. In the 50-2.5-47.5 glass (shown in the left-hand column of Figure 8), the $Q^1(m\text{Al})$ phosphorus (−7.1 ppm) and the $Q^1(0\text{Al})$ phosphorus (+1.6 ppm) resonances are proportionately reduced in the TRAPDOR experiment while the $Q^2(0\text{Al})$ phosphorus resonance (−18.7 ppm) displays a less pronounced effect. This implies that the TRAPDOR effect between ^{23}Na and ^{31}P is greater for the $Q^1(m\text{Al})$

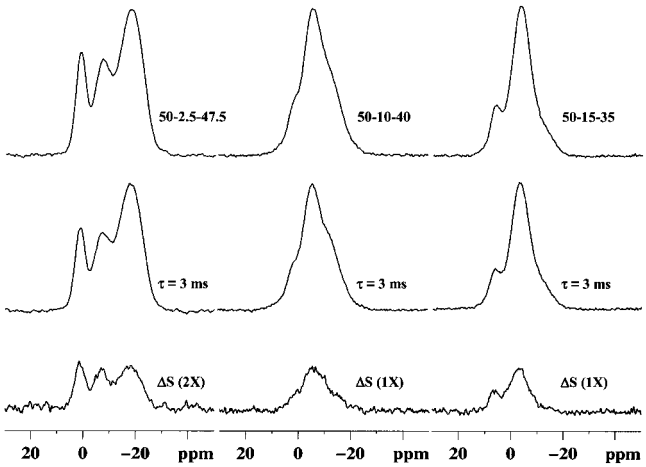

Figure 8. $^{31}P/^{23}Na$ TRAPDOR results of the 50-2.5-47.5 (left), 50-10-40 (middle), and 50-15-35 (right) NAP glasses. The top spectra are acquired without irradiation of the ^{23}Na nuclei. The spectra in the center were acquired with 50 kHz of irradiation applied to the ^{23}Na nuclei. The bottom spectra show the TRAPDOR difference, ΔS, $\tau = 3$ ms resulting from each experiment.

and $Q^1(0Al)$ environments than for the $Q^2(0Al)$ environments, perhaps suggesting a larger dipolar coupling as a result of either a shorter ^{23}Na to ^{31}P bond distance or an increase in the number of ^{23}Na affecting the ^{31}P environment. For the 50-10-40 and 50-15-35 glasses all the phosphorus environments appear proportionally affected.

Discussion

Utilizing these NMR results, a better understanding regarding the MRO and structural evolution occurring in the near-metaphosphate base glass as a function of aluminum incorporation can be detailed. The structure of the sodium metaphosphate glass (50-0-50) consists of chains of $Q^2(0Al)$ phosphate tetrahedra having moderate length terminated by $Q^1(0Al)$ end groups.[6,8,19] While the RFDR experiment performed on this sample does not definitively rule out the concomitant existence of $Q^2(0Al)$ phosphate ring structures and $Q^1(0Al)$ diphosphate regions, it does clearly define the $Q^2(0Al)$ and $Q^1(0Al)$ chain motif as the preferred structure.

Incorporating aluminum into the sodium near-metaphosphate glass results in the formation of aluminophosphate environments. The linear behavior of the $^{31}P/^{27}Al$ TRAPDOR effect shown in Figure 5b strongly argues against the possibility of Al or Al/Na segregation. If such segregation were occurring, then the Al−P interaction would show a less pronounced decrease. This linear result also suggests that variations in the TRAPDOR efficiency due to changes in the Al coordination number do not appear very large. The predicted pathways for aluminum integration are primarily 2-fold: (1) either the aluminum replaces a sodium atom on one of the nonbridging oxygens (NBO) associated with a $Q^2(0Al)$ or $Q^1(0Al)$ tetrahedra or (2) the aluminum incorporates into the glass structure by breaking a P−O−P bond within the melt and forms a bridging P−O−Al bond, with the $Q^2(0Al)$ tetrahedral species becoming a $Q^1(mAl)$ $m = 1, 2$ tetrahedra. Aluminum integration via the first pathway is expected to increase the shielding on the phosphorus nucleus, thereby making the ^{31}P chemical shift more negative.[58] This trend is not observed in the ^{31}P NMR spectra following the addition of aluminum (see Figure 2). Formation of P−O−Al bonds via the second pathway is predicted to decrease the shielding on the phosphorus nucleus, thereby making the chemical shift more positive. The 1D ^{31}P and $^{31}P/^{27}Al$ and $^{31}P/^{23}Na$ TRAPDOR NMR results support this as the dominant integration pathway. In the 50-0-50 base glass 90% of the phosphorus tetrahedra reside in a $Q^2(0Al)$ environment (see Table 1). After the addition of 2.5 mol % aluminum, the relative percentage of $Q^2(0Al)$ environments is reduced to 70%, the amount of new $Q^1(mAl)$ environments created is 20%, and the phosphorus in $Q^1(0Al)$ tetrahedra remains unchanged at 10%. The conversion of $Q^2(0Al)$ to $Q^1(mAl)$ tetrahedral species appears to be the dominant structural variation for glass compositions through 50-7.5-42.5 (i.e., $P_{Q^2(0Al)} + P_{Q^1(mAl)} = 90\%$, see Table 1). In fact, $P_{Q^2(0Al)} + P_{Q^1(mAl)} \cong 90\%$ through the 50-12.5-37.5 composition, implying that the Al incorporation involves primarily the formation of $Q^1(mAl)$ species between 7.5 and 12.5 mol % aluminum as well and that the relative concentration of $Q^1(0Al)$ species are not largely affected by the addition of Al ($P_{Q^1(0Al)} \approx 10\%$). This conclusion is supported by the fact that the ^{31}P NMR resonances between 0 and −14 ppm continue to show dipolar coupling to aluminum in the $^{31}P/^{27}Al$ TRAPDOR experiments, while the $Q^1(0Al)$ resonance produces a null ΔS spectrum (see Figure 6).

The assignment of these new ^{31}P NMR resonances has remained controversial.[58,57,9,59,41] In the Dollase et al. investigation of orientationally disordered crystals (ODC) for the $Na_{3-3x}Al_xPO_4$ series, the ^{31}P NMR resonance between −3.5 and −5 ppm was assigned to a $Q^1(2Al)$ phosphate tetrahedral species.[58] Brow et al. thus suggested that the resonance forming between −8 and −11 ppm in an analogous amorphous aluminophosphate system might be attributed to $Q^1(2Al)$ environments.[57] One scenario they proposed was that two $-O^-Na^+$ species are replaced by two −OAl(6) species on a $Q^1(0Al)$ tetrahedron, thereby causing the displacement of the chemical shift to more negative values relative to the approximately +2 ppm for $P(OP)(O^-Na^+)_3$. The $^{31}P/^{27}Al$ and $^{31}P/^{23}Na$ TRAPDOR results presented in this manuscript, however, show that the initial aluminum incorporates not by replacing $-O^-Na^+$ species but, rather, by replacing P−O−P environments with P−O−Al environments within the melt. To the best of our knowledge, this is the first experiment showing that added aluminum incorporates preferentially within the $Q^2(0Al)$ chain rather than to terminal $Q^1(0Al)$ species. As it seems unlikely that the dominant integration pathway would be directly from $Q^2(0Al)$ to $Q^1(2Al)$ at only 2.5 mol % aluminum, we attribute the new phosphorus resonance at −7.1 ppm to the formation of $Q^1(1Al)$ species. From the $^{31}P/^{27}Al$ TRAPDOR results, these species show dipolar coupling with the added aluminum, and the upfield tailing of this resonance in the TRAPDOR ΔS spectrum implies that either a small amount of another $Q^1(mAl)$ species exists or that the $Q^2(0Al)$ species are also dipolar coupled to the aluminum (see Figure 6). Interestingly, the $Q^1(0Al)$ species are completely eliminated in the difference spectrum of the 50-2.5-47.5 glass, implying that they have no dipolar

coupling with the added aluminum. The lack of $Q^0(m\text{Al})$ formation at low Al concentrations also demonstrates that preferential Al coordination to $Q^1(0\text{Al})$ end groups does not occur.

The 50-2.5-47.5 glass has an O/P ratio close to 3.1, and its ^{27}Al MAS NMR spectrum shows 86% of the aluminum as having octahedral coordination (see Table 2). Thus, the proposal of the ^{31}P resonance at −7.1 ppm to a $Q^1(1\text{Al})$ environment leaves a local charge balancing question. Namely, if the attached aluminum in an $Q^1(1\text{Al})$ environment is Al(6), then one of the terminal oxygens will be underbonded and require coordination to multiple sodium ions to obtain charge neutrality. Even though a significant fraction of Al(5) and Al(4) are present in all compositions to assist in charge balancing, previous work on similar glass systems have often submitted that the resonance between −6 and −11 ppm is due to $Q^1(2\text{Al})$ species, which are charge neutral when all of the NNN aluminum nuclei are Al(6).[9,41,57] Recent work by Belkébir et al., however, proposes that a disproportionation of diphosphate species into triphosphate and monophosphate ions cross-linked by aluminum atoms whose average coordination increases accounts for the ^{31}P resonance near −7 ppm.[59] As their solution ^{31}P NMR results reveal a large proportion of diphosphate still present in the glass with an O/P ratio of 3.5 (50-10-40), it does not seem reasonable to assign the resonance at approximately −7 ppm to a $Q^0(m\text{Al})$ or $Q^2(0\text{Al})$ species. From the deconvolution of their solid-state ^{31}P MAS NMR spectra, they propose that the resonances at −6.8 and approximately −16 ppm belong to $P(OP)(OAl)(ONa_y)_2$ (i.e., $Q^1(1\text{Al})$), and $P(OP)(OAl)_2(ONa_y)$ species (i.e., $Q^1(2\text{Al})$), respectively. Here, the value of "*y*" is not obvious to specify as the coordination of the oxygen does not remain equal to 2.[59] The presence of multiple cationic environments, in conjunction with the existence of Al(4) and Al(5) environments, helps address the charge balancing question and support our assignment of the ^{31}P resonance at −7.1 ppm to a $Q^1(1\text{Al})$ species.

With the addition of 10 mol % aluminum, the $Q^1(1\text{Al})$ environment dominates the phosphorus spectrum and the preferred coordination of aluminum is changing from Al(6) to Al(4), with ≈20% remaining as Al(5). This change in coordination coincides with the increase in the O/P ratio of the glass. When O/P = 3.0 (50-0-50 glass), the preferred phosphate structure is the metaphosphate Q^2 chain. When O/P = 3.5 (50-10-40), the preferred structure is expected to be pyrophosphate.[5] While a crystalline $Q^1(3\text{Al})$ structure can support three Al(6) environments and remain charge balanced,[54] if the O/P ratio becomes >3.5, the aluminum must take on a lower coordination state to keep the system charge neutral.[9] Deconvolution of the 50-10-40 ^{31}P MAS spectrum yields chemical shift values of −12.0, −5.4, and +1.6 ppm (see Table 1). The change in the chemical shift value for the $Q^1(1\text{Al})$ species is +1.7 ppm versus the 50-2.5-47.5 glass, while the change to the $Q^1(0\text{Al})$ species is negligible. The ^{31}P/^{27}Al TRAPDOR experiment, Figure 6, singles out only the −12.0 and −5.4 ppm environments as being dipolar coupled to aluminum. Once again, the $Q^1(0\text{Al})$ species are absent from the TRAPDOR difference spectrum, ΔS. Knowing that additional NNN aluminum atoms will make the chemical shift of $Q^1(1\text{Al})$ phosphorus more negative,[58] one plausible integration scenario occurring at the pyrophosphate transition point (O/P = 3.5) is that a portion of the $Q^1(1\text{Al})$ species are modified to $Q^1(2\text{Al})$ species while the remaining $Q^2(0\text{Al})$ species form $Q^1(1\text{Al})$ species. Both Belkébir et al.[59] and Egan et al.[41] also note the existence of $Q^1(2\text{Al})$ species for an O/P ratio of ≈3.5. Egan et al., however, who acquired much of their data using cross-polarization from ^{27}Al to ^{31}P, attribute the ^{31}P NMR resonance they see at approximately −11 ppm to $Q^0(3\text{Al})$ species and the resonance at approximately −6 ppm to $Q^1(2\text{Al})$ species. A $Q^0(3\text{Al})$ species is made charge neutral with one Al(6) and two Al(4) NNN, while a $Q^1(2\text{Al})$ species is made charge neutral with two Al(6) NNN.[9] In the 2D CPMAS correlation spectrum of Egan et al.[41] both sites show coordination to the Al(4) and Al(6) aluminum nuclei, but only the $Q^1(2\text{Al})$ species shows coordination to Al(5) aluminum. Their ability to assign each phosphorus resonance to a specific coordinated aluminum nuclei is a very nice feature of the ^{27}Al to ^{31}P CPMAS technique. As stated above, though, we assign the ^{31}P resonance at −12 ppm in our spectrum to the $Q^1(2\text{Al})$ species. At or below an O/P ratio of 3.5, the creation of an alumino orthophosphate species, for example, $Q^0(3\text{Al})$, does not appear to be a prominent reaction. Actually, the ODC investigation done by Dollase et al. found phosphorus nuclei in $Q^0(3\text{Al})$ environments to be more shielded and to resonate at approximately −15 ppm.[58]

At 15 mol % aluminum the amount of Q^2 tetrahedra are negligible. We attribute the phosphorus resonances observed at −9.5 ppm (24%), −2.7 ppm (62%), and +6.3 ppm (14%) to $Q^1(2\text{Al})$, $Q^0(2\text{Al})$,[58] and $Q^0(1\text{Al})$[58] environments, respectively. As all these environments have aluminum as the NNN, the ^{31}P/^{27}Al TRAPDOR difference spectrum displays the expected dipolar coupling between ^{27}Al and ^{31}P in all of them (see Figure 6). Interestingly, our ^{31}P/^{27}Al TRAPDOR results have shown throughout that all of the new ^{31}P MAS resonances observed with increasing aluminum concentration are dipolar coupled to aluminum.

The constant ^{31}P/^{23}Na TRAPDOR decay observed in Figure 7 demonstrates that the ^{23}Na−^{31}P environment is not significantly impacted by the addition of aluminum. If there were extensive replacement of ^{23}Na by ^{27}Al within the ^{31}P local environments, the TRAPDOR decay curves would reveal the variations. This supports our conclusions based on the previously discussed ^{31}P/^{27}Al TRAPDOR results that at lower aluminum concentrations P−O−Al environments are formed in place of P−O−P environments within the melt without the apparent displacement of existing $-O^-Na^+$ environments. The ^{31}P/^{23}Na TRAPDOR results in Figure 8 also reveal that all of the ^{31}P resonances are dipolar coupled to ^{23}Na. As the molar percent of sodium remains fixed at 50 throughout our entire glass series, it is not too surprising that all of the ^{31}P environments show ^{23}Na dipolar coupling. The invariant sodium−phosphorus environment implies that large structural changes in the Na−P bonding do not occur for this glass series and that any observed changes in the physical properties of

(59) Belkébir, A.; Rocha, J.; Esculcas, A. P.; Berthet, P.; Gilbert, B.; Gabelica, Z.; Llabres, G.; Wijzen, F.; Rulmont, A. *Spectrochim. Acta A* **1999**, *55*, 1323.

the glass must be a result of changes in the Al−P and P−O bonding environments.

Conclusions

On the basis of the multinuclear NMR experimental results, we propose a structural modification pathway for the $x Al_2O_3 \cdot 50Na_2O \cdot (50-x)P_2O_5$ ($0 \le x \le 17.5$) glass series studied using the $Q^2(0Al) \rightarrow Q^1(1Al) \rightarrow Q^1(2Al) \rightarrow Q^0(2Al)$ and $Q^1(0Al) \rightarrow Q^0(1Al)$ structural evolution schemes. When the molar percent of aluminum is lower than 10 (O/P ratio < 3.5), the preferred structures of the glass are modified metaphosphate $Q^2(0Al)$ chains.[5] Adding aluminum to the glass composition results in the formation of P−O−Al environments and the reduction of P−O−P environments, for example, $Q^2(0Al) \rightarrow Q^1(1Al)$. As the amount of $Q^2(0Al)$ species reduces further, an additional phosphorus environment is created, $Q^1(2Al)$. The $Q^1(2Al)$ environment becomes the dominant feature in the ^{31}P spectrum at ≈10 mol % aluminum, while the concentration of the $Q^1(0Al)$ environments does not appear to be significantly affected by the added aluminum until after the O/P ratio is greater than 3.5. Only at 15 and 17.5 mol % aluminum do we finally see the $Q^1(0Al) \rightarrow Q^0(1Al)$ evolution occur. We believe it is the creation of these P−O−Al cross-linking environments within the glass network, not modification of the P−O−Na environments, that are responsible for the increased durability and other physical changes noted by Brow et al. in their earlier analysis of this glass series.[9]

For O/P ratios greater than 3.5 (mol % Al > 10) the preferred coordination of aluminum is tetrahedral, Al(4), and the amount of phosphorus residing in $Q^2(0Al)$ environments are negligible. In the melt we propose that with increasing aluminum concentration the $Q^2(0Al)$ species are replaced by $Q^1(1Al)$ species, followed by the formation of $Q^1(2Al)$ species. Beyond 10 mol % aluminum, the $Q^0(2Al)$ alumino orthophosphate species is the dominant phosphorus environment. Finally, when the molar percent of aluminum is greater than 12.5, the $Q^1(0Al)$ tetrahedral species are replaced as well, with the formation of $Q^0(1Al)$ environments.

The NMR results presented here demonstrate that with combination of $^{31}P/^{27}Al$ and $^{31}P/^{23}Na$ TRAPDOR experiments with classical 1D ^{31}P and ^{27}Al MAS NMR experiments, more structural information about a glass system can be obtained, including the relative distribution of modifying cations with respect to the phosphate backbone. Such structural information also provides insight for analyzing many of the glass dissolution mechanisms that are presently being investigated in our laboratory.

Acknowledgment. The authors would like to express their thanks and appreciation to Dr. Richard Brow for his careful reading and suggestions for making this manuscript more complete. Sandia is a multiprogram laboratory operated by Sandia Corporation, a Lockheed Martin Company for the United States Department of Energy under Contract DE-AC04-94AL85000.

CM000717L